Separation Science and Technology
Publication details, including instructions for authors and subscription information:
http://www.informaworld.com/smpp/title~content=t713708471

Modification of Nanofiltration Membranes by Surface-Initiated Atom Transfer Radical Polymerization for Produced Water Filtration

Namrata Tomer[a]; Subrata Mondal[b]; Daniel Wandera[a]; S. Ranil Wickramasinghe[b]; Scott M. Husson[a]
[a] Department of Chemical and Biomolecular Engineering and Center for Advanced Engineering Fibers and Films, Clemson University, Clemson, SC, USA [b] Department of Chemical and Biological Engineering, Colorado State University, Fort Collins, CO, USA

To cite this Article Tomer, Namrata , Mondal, Subrata , Wandera, Daniel , Wickramasinghe, S. Ranil and Husson, Scott M.(2009) 'Modification of Nanofiltration Membranes by Surface-Initiated Atom Transfer Radical Polymerization for Produced Water Filtration', Separation Science and Technology, 44: 14, 3346 — 3368
To link to this Article: DOI: 10.1080/01496390903212540
URL: http://dx.doi.org/10.1080/01496390903212540

Separation Science and Technology, 44: 3346–3368, 2009

ISSN: 0149-6395 print/1520-5754 online
DOI: 10.1080/01496390903212540

Taylor & Francis
Taylor & Francis Group

Modification of Nanofiltration Membranes by Surface-Initiated Atom Transfer Radical Polymerization for Produced Water Filtration

Namrata Tomer,[1] Subrata Mondal,[2] Daniel Wandera,[1] S. Ranil Wickramasinghe,[2] and Scott M. Husson[1]

[1]Department of Chemical and Biomolecular Engineering and Center for Advanced Engineering Fibers and Films, Clemson University, Clemson, SC, USA

[2]Department of Chemical and Biological Engineering, Colorado State University, Fort Collins, CO, USA

Abstract: Poly(N-isopropylacrylamide) and poly(N-isopropylacrylamide-*block*-ethylene glycol methacrylate) were grafted from commercial polyamide thin-film composite nanofiltration membranes using surface-initiated atom transfer radical polymerization. The results from Fourier-transform infrared spectroscopy confirmed the successful grafting of both polymers from the membrane surfaces. Contact angle measurements were done to illustrate the temperature responsive wettability of the modified membrane surfaces. Modified membranes were used in flux measurements of wastewater produced during coal bed methane gas exploration. The degree of fouling of the original and the modified membranes was examined by pure water flux recovery measurements after produced water filtration and a temperature-controlled water rinse.

Keywords: ATRP, membrane fouling, PNIPAAm, PPEGMA, surface modification

Received 28 August 2008; accepted 14 April 2009.

Address correspondence to Scott M. Husson, Department of Chemical and Biomolecular Engineering, Clemson University, 126 Earle Hall, Clemson, SC 29634-0909, USA. Tel.: +1 (864) 656-4502; Fax: +1 (864) 656-0784. E-mail: shusson@clemson.edu

INTRODUCTION

Oil and gas are the world's main energy sources, and their production is an important issue. High oil and gas prices coupled with our ever increasing energy needs will drive the development and exploration of new oil and gas sources, e.g., oil shale and coal bed methane. During the production of oil and gas, certain unfavorable effects impact the environment. Produced water is a by-product from oil and gas exploration that contributes significantly to these unfavorable effects (1), as much of the produced water generated today is treated as waste. Due to contact with hydrocarbon products and geologic formations in underground basins, produced water usually contains elevated concentrations of inorganic and organic contaminants (2).

Produced water is separated from the hydrocarbons, treated to remove as much oil as possible, and is then either re-injected into a reservoir, discharged into a surrounding body of water, or used in land applications. Reinjection is an expensive option for oil and gas producers and can be done only when the underground structure can accommodate the water. Surface discharge can cause stream bank erosion and changes in natural vegetation, and can contaminate drinking water or irrigation water supplies either underground or on the surface. In addition, the salinity of the produced water can vary from almost fresh to saturated, depending upon the source geology and production process. In land applications, the salt commonly found in produced water can make soil less permeable to air and water and reduce the availability of nutrients in the soil. Due to their complex chemical composition (oil, salt, heavy metals, radionuclides, and treatment chemicals) and their large production volumes, produced waters that are surface discharged are targeted by the organizations responsible for environmental protection, which have established strict regulations on the maximum levels of heavy metals and other impurities allowed in water (3).

The treatment of produced water requires de-oiling and demineralization. The use of membrane filtration processes such as nanofiltration and reverse osmosis offers potential advantages over more traditional methods for the treatment of produced waters (4). However, a major obstacle associated with membrane-based treatment of produced water is the flux decline due to concentration polarization and subsequent membrane fouling. Concentration polarization refers to the formation of a high concentration boundary layer of rejected species at the membrane surface, while membrane fouling is due to the deposition of rejected species on the membrane surface. Membrane fouling not only decreases the membrane permeability, but also shortens membrane life due to the aggressive chemical usage necessary for cleaning. When

cleaning becomes ineffective, the membrane needs to be replaced. As a result, membrane fouling is one of the most significant economic challenges faced in membrane filtration operations.

Membrane fouling due to interactions between suspended and dissolved solutes and the membrane surface can be both reversible and irreversible. Mass accumulation on a membrane surface can be reversible if the matter is accumulated but stays dispersed; that is, it does not bind directly to the surface, and a reduction in the applied pressure reduces the concentration polarization by diffusion away from the surface (5,6). Thus, membrane fouling may possibly be controlled by changing the membrane surface chemistry. Previous investigations have demonstrated that, generally speaking, increasing membrane surface hydrophilicity can inhibit membrane fouling in water/wastewater treatment operations (7).

In the present study, poly(N-isopropylacrylamide) (PNIPAAm) and PNIPAAm-*block*-poly(ethylene glycol methacrylate) (PPEGMA) nanolayers were grafted from commercial polyamide thin-film composite nanofiltration membranes via surface-initiated atom transfer radical polymerization (ATRP). The use of ATRP for the modification of polymeric membrane surfaces is preferred (8–14) in contrast to other controlled radical polymerization techniques, as it is versatile with respect to the selection of monomers and reaction conditions (15–21). ATRP can be done in the presence of water (8–10,15,16,20) often at room temperature, and, as a catalyst-activated process, can be done in-situ for modification to membrane modules. Surface-initiated ATRP leads to grafted polymers with higher chain densities than methods that graft end-functionalized polymer chains onto a surface. One limitation relevant to this study is that controlled polymerization of acrylamides by ATRP in organic media is elusive (22–25); however, growing polymers of substituted acrylamides with controlled chain densities and molecular weights from surfaces in aqueous media have been reported (20,26–28).

PNIPAAm exhibits a lower critical solution temperature (LCST) at 32°C in aqueous solution that was first reported by Heskins and Guillet (29) using a Flory-Huggins analysis. Below the LCST, PNIPAAm chains hydrate to form a random coil structure, while, above the LCST, PNIPAAm chains form a collapsed globular structure. The collapsed state has more hydrophobic character than the extended coil. As the physical structures and properties of PNIPAAm are readily controlled by changing the system temperature, it is used widely to prepare stimuli-responsive materials (30–33). Attaching a PNIPAAm block to the membrane makes it temperature responsive.

A common approach to modify water-treatment membranes is to physically coat (34) or chemically graft hydrophilic polymers (35) that increase membrane wettability and reduce their potential to foul. It

appears that intermediate values of wettability (water contact angles of ~35–42°) yield good antifouling behavior (36,37). Among the polymers that satisfy this condition is PEG. Our group has previously shown that PPEGMA can be grown by surface-initiated ATRP from membranes (9) and used as a non-fouling polymer to prevent surface attachment of microorganisms and proteins (38). Attaching a PPEGMA block to the membrane reduces its fouling tendency.

Thus, our goal in this work was to modify nanofiltration membrane surfaces with block copolymer nanolayers comprising a temperature-responsive block and a foul-resistant block in order to limit fouling during filtration of coal bed methane produced water, and to provide a chemical-free alternative to detach any foulants that do accumulate on the surface.

EXPERIMENTAL

Materials

Commercially available, polyamide thin-film composite membranes (FILMTEC^{TM} NF 270) were provided by Dow. The polyamide layer in this membrane is created by interfacial polymerization of piperazine and benzene-1,3,5-tricarbonyl trichloride (39).

Chemicals were used as received from Aldrich unless noted otherwise; they were aluminum oxide (150 mesh), azobisisobutyronitrile (AIBN, 98%), 2-bromoisobutyryl bromide (2-BIB, 98%), 2-bromo-2-methylpropionic acid (BPA, 98%), copper(I) chloride, (99.995 + %), copper(II) chloride (99.99%), glycidyl methacrylate (95%), hydrogen peroxide (30%, v/v in water, VWR), 1,1,4,7,7-pentamethyldiethylenetriamine (PMDETA, 98%), sulfuric acid (95–98%, EMD Chemicals, Inc.), triethylamine (TEA, 99.5%). Solvents were ACS reagent or HPLC grade; they were acetonitrile (anhydrous, 99.9%), ethanol (99.5%), methanol (99%), methyl ethyl ketone (MEK, 99.6%), and water.

Poly (ethylene glycol) methacrylate (PEGMA) macromonomer (M_n ~ 360 g/mol) was dehibited by passing through a neutral aluminum oxide column. N-Isopropylacrylamide (NIPAAm, 97%) was purified by recrystallization from n-hexane.

Silicon wafers (Silicon Quest International) were used as substrates for kinetic studies. The wafers were cleaned for 30 minutes in deionized water using an ultrasonic bath and then treated for 1 h at 60°C with a piranha solution (freshly made 3:1 (v/v) mixture of concentrated sulfuric acid and hydrogen peroxide (30%). (Precaution: Use in limited quantities and avoid contact with organic compounds, which react aggressively with

Table 1. Specifications of coal bed methane produced water measured at 23.1°C

Total dissolved solids (TDS)	722 ppm
Total organic carbon (TOC)	68.8 mg/L
Conductivity	1448 μS
pH	8.52

this mixture.) The wafers were rinsed with deionized water and dried by a stream of nitrogen.

Coal Bed Methane (CBM) produced water (PW) was obtained from Walsenburg, CO. Table 1 gives the PW specifications.

Methods

Surface Functionalization of Membranes with ATRP Initiator

The polyamide thin-film composite membranes were immersed in a solution of 50% (v/v) ethanol, 45% HPLC water, and 5% sulfuric acid for 24 hours. This acid treatment step hydrolyzes amide bonds to create amine and acid groups (40). Next, the membranes were rinsed thoroughly with water, and then equilibrated with anhydrous acetonitrile.

The membranes were immersed in a solution of 2-bromoisobutyryl bromide (2 mM), triethylamine (2 mM), and 20 mL of anhydrous acetonitrile for 2 hours at room temperature to immobilize the initiator by reaction with the amine groups generated on the polyamide membrane in the previous step. After reaction, the initiator-functionalized membranes were removed from the reaction mixture and washed thoroughly with acetonitrile and then HPLC water.

Surface-Initiated ATRP from Membrane Surfaces

Surface-initiated ATRP was done to graft PNIPAAm, PPEGMA, and PNIPAAm-*block*-PPEGMA nanolayers from the initiator-functionalized membranes. Table 2 gives the details of the types of modifications and the times of polymerization used to modify the membranes in this study. PNIPAAm (0.1 M), CuCl (0.5 mM), $CuCl_2$ (0.10 mM), and PMDETA (1.0 mM) were added to a solvent mixture comprising 20 mL HPLC water and 0.2 mL methanol. The mixture was deoxygenated using three freeze-pump-thaw cycles. High-purity nitrogen was used to fill the sample headspace following vacuum evacuation. All polymerization steps were

Table 2. Notations for modified membranes

Polymer modifier (polymerization duration)	Sample notation
PNIPAAm (24 h)	NF 270-M1
PNIPAAm-*block*-PPEGMA (10 h for PNIPAAm + 10 h for PPEGMA)	NF 270-M2
PNIPAAm-*block*-PPEGMA (5 h for PNIPAAm + 5 h for PPEGMA)	NF 270-M3
PNIPAAm-*block*-PPEGMA (2 h for PNIPAAm + 2 h for PPEGMA)	NF 270-M4

carried out at room temperature in an oxygen-free glove box. Membranes grafted with PNIPAAm were removed from the polymerization solution at defined times and immediately submerged into a solution of $Cu(II)Cl_2$ (5 mM) and PMDETA (5 mM) in 10 mL water to ensure that growing radical chains were end-capped with the halide. These membranes were then rinsed with HPLC water.

PPEGMA brushes were grafted from the PNIPAAm-modified membranes. PEGMA (0.2 M), CuCl (1 mM), $CuCl_2$ (0.20 mM), and PMDETA (2 mM) were added to a solvent mixture comprising 20 mL HPLC water and 0.2 mL methanol. The mixture was deoxygenated, the reaction flask was transferred to the glove box, and a PNIPAAm-modified membrane was placed in the polymerization solution for a defined time. The block copolymer-modified membrane was removed from the reaction mixture and washed thoroughly with HPLC water. The polymerization time was varied to adjust the masses of PNIPAAm and PPEGMA grafted from the membrane surfaces.

Surface-Initiated ATRP from Silicon Wafers

Surface-initiated polymerization from cleaned silicon surfaces was done by first depositing a reactive layer of poly(glycidyl methacrylate) (PGMA). The PGMA with $M_n = 84{,}000$ g/mol and polydispersity index of 3.4 was prepared by radical polymerization of glycidyl methacrylate in MEK at 60°C using AIBN as an initiator. PGMA was deposited on the silicon surface by dip coating from a 0.2 wt.% PGMA solution in MEK. The details were presented by Lui et al. (41). The PGMA-coated silicon surfaces were annealed at 110°C for 30 minutes under vacuum. To add ATRP initiator groups, the surfaces were then placed in a Schlenk tube with 1 g of BPA. The Schlenk tube was evacuated to 130 Pa and placed in an oven at 110°C for 18 h to react the vapor phase BPA with the epoxide groups of PGMA. After reaction, the surfaces were soaked

in MEK for 10 min and rinsed with MEK three times. Polymerization of PNIPAAm from the PGMA coated silicon substrates was carried out using the same conditions used for the membrane surface modification. A kinetic study was done to measure the PPNIPAAm layer thicknesses as a function of the polymerization time.

Physicochemical and Performance Characterization

Attenuated Total Reflectance Fourier-Transform Infrared Spectroscopy (ATR-FTIR)

ATR-FTIR spectra were collected for the polymer-modified and unmodified membranes to analyze changes in the membrane surface chemistry. Instrument details and operating parameters were given previously (8).

Atomic Force Microscopy

AFM images of modified and unmodified membranes in deionized water were obtained in contact mode using a Multi Mode AFM (Veeco). Surface roughness was calculated using NanoScope Software Version 5.12.

Water Contact Angle Goniometry

Static water contact angles were measured for all membrane surfaces using a KRÜSS DSA10 contact angle measuring system. The sessile drop method was used with HPLC grade water, and contact angles were determined using the Young-Laplace fitting method. Membranes were placed in a temperature-controlled test chamber mounted on the sample stage of the instrument. The chamber has a glass window for viewing and a small opening at the top for introducing the dispenser needle. The temperature of the testing chamber was controlled by continuous circulation of water using a Haake DC10 thermostatted circulator bath. A few minutes after the temperature of the membranes was stabilized, a 3 μl drop of water was placed onto the surface of the membrane and the contact angle was recorded immediately. This process was repeated at a minimum of five spots on each membrane surface, and the mean values are reported. Error bars represent ± 1 standard deviation from the mean.

Ellipsometry

Polymer layers grown from silicon substrates were characterized by multi-angle ellipsometry. Details of the instrument and methodology were given

previously (38). Dry layer thicknesses were measured at five separate spots on each sample with an assumed refractive index of 1.525 for PGMA and 1.5 for BPA (41). The assumed refractive index was 1.46 for PNIPAAm brushes less than 50 nm thick, and 1.47–1.49 for thicker PNIPAAm brushes (42). A multilayer Cauchy model (Igor Pro Software) was used to fit ellipsometric data in order to determine layer thicknesses.

Water Flux Measurement

Scheme 1 shows the experimental steps for the water flux measurements. Membranes were pre-equilibrated in DI water for 3 h prior to use. Water flux measurements with unmodified and surface-modified membranes were carried out using a dead-end filtration cell (YT30 142 HW, Millipore Corp., Bedford, MA). The membrane diameter was 140 mm. The feed was pressurized using a nitrogen cylinder attached to the feed chamber. The feed volume was 500 mL. Each membrane was used to filter DI water starting at 410 kPa with increasing increments of 70 kPa up to 690 kPa. Permeates were collected for 5 min. Two minutes were allowed in between the pressure increases to stabilize the pressure inside the filtration system. The produced water was filtered using the same method soon after the DI water was filtered. After produced water filtration, the membrane surfaces were rinsed with warm water (40°C) or room temperature water and the DI water flux was re-measured. The filtration flux of each membrane at all pressures was calculated using Eq. (1), where V is the volume of permeate, A is the area, and t is the time.

$$\text{Flux} = (\text{V}/\text{A} \cdot \text{t}) \tag{1}$$

The variation of the conductivity and TDS of the permeate was determined using a handheld conductivity/TDS meter (Oakton Instruments, Vernon Hills, IL).

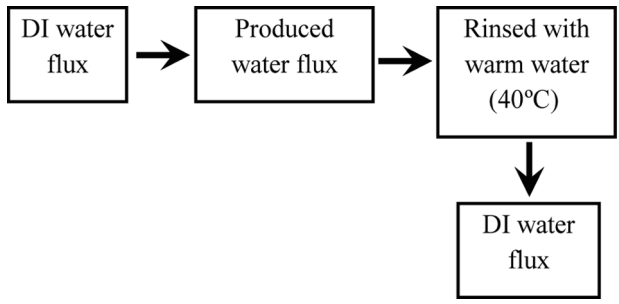

Scheme 1. Experimental steps for water flux measurements.

RESULTS AND DISCUSSION

Characterization of Membrane Surfaces

Figure 1 presents the ATR-FTIR spectra of unmodified and PNIPAAm-*block*-PPEGMA modified NF 270 polyamide thin-film composite membranes. Following polymerization, an increase is seen in the intensity of peaks at 1630 and 1580 cm^{-1}, which are characteristic peaks assigned to the amide carbonyl groups and N–H bending of PNIPAAm. Also increased are the peaks in the range of 1366–1466 cm^{-1}, which are assigned to symmetrical and asymmetrical deformation bands associated with the isopropyl group in PNIPAAm (43). A new peak appears at 1710 cm^{-1} that is attributed to the carbonyl group in the methacrylate backbone of PPEGMA. Another peak appears around 3500 cm^{-1}, assigned to the stretching of the non-hydrogen bonded –OH groups in PEG (44). And there are increases in the intensities of peaks in the region of aliphatic vibration 2860–2960 cm^{-1}. Finally, overall increases in peak intensities for NF 270-M2 (spectrum C) relative to NF 270-M3 (spectrum B) support the expected outcome that a longer polymerization time leads to a higher mass of grafted polymer.

AFM was employed to evaluate the variations in surface morphology of NF 270 membranes after PNIPAAm and PPEGMA grafting. Measurements were done in water, such that the grafted polymer chains

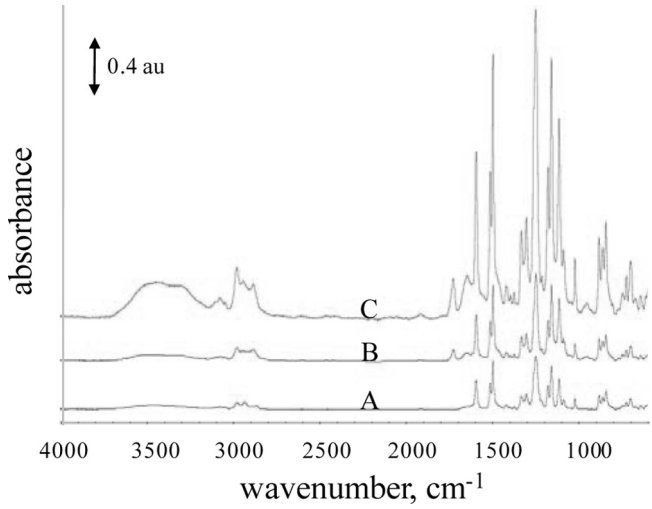

Figure 1. ATR-FTIR spectra for (A) unmodified NF 270 membrane, (B) NF 270-M3, (C) NF 270-M2.

would be solvated. The root-mean-square roughness values increased from 4 ± 2 nm for unmodified membrane surfaces to 9 ± 2 nm for NF 270-M3 and 13 ± 2 nm for NF 270-M2. Control tests were done to measure the RMS roughness values for membranes following acid treatment and initiator incorporation. The roughness values did not change following these steps. This result indicates that the increased roughness of the membrane surface was caused by the introduction of the grafted polymer nanolayers. Often, surface-initiated polymerization will make rough surfaces smoother (45–47). And, generally speaking, controlled polymer growth by surface-initiated ATRP produces a smoother topography than other conventional radical polymerization methods, especially when producing ultrathin polymer films (48). Previously, we observed decreased RMS roughness values in the dry state following the modification of microporous membranes by ATRP (10,11). It was, therefore, unexpected to see an increase, albeit small, in the surface roughness following polymerization. It is possible that this increase in roughness is associated with uncontrolled growth of PNIPAAm in the first step. Uncontrolled growth is common for acrylamide-based polymers grown by ATRP (22–25), and our results (vide infra) from the kinetic studies of surface-initiated ATRP of PNIPAAm suggest lack of control. This lack of control reduces the reinitiation efficiency for PPEGMA and otherwise increases the chain length polydispersity index. A broad polydispersity in chain lengths may explain the increase in surface roughness. Nevertheless, the RMS roughness values measured in this work (9 nm) are significantly lower than those reported for water-treatment membranes prepared by physical coating with polyether-*block*-polyamide (>48 nm) (34) and grafting of preformed PEG chains (93 nm) (35). This result is particularly important since earlier studies have shown that increasing surface roughness leads to increased fouling and higher adsorption of organic compounds (49).

Thermo-Responsiveness of Nanolayer Modified Membrane Surfaces

Contact angle measurements were done to assess the changes in the wetting characteristics of membrane surfaces before and after modification. The static water contact angle of unmodified NF 270 was measured to be $35 \pm 4°$. After PNIPAAm grafting, the membrane surfaces became more hydrophobic, as seen by an increase in the contact angle to $61 \pm 2°$. Subsequent grafting of PPEGMA to form PNIPAAm-*block*-PPEGMA nanolayers on the membrane surface led to a reduced contact angle of $49 \pm 2°$. These water contact angle results are consistent with published data for PNIPAAm and PPEGMA (50,51).

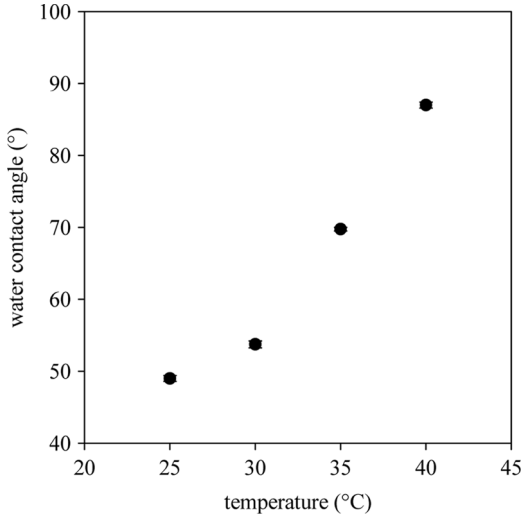

Figure 2. Temperature dependence on static water contact angles of modified NF 270-M2.

Figure 2 shows the water contact angle as a function of temperature on PNIPAAm-*block*-PPEGMA modified NF 270. The contact angle increases with temperature, indicating that the surface becomes more hydrophobic. This result can be explained by differences in the intermolecular and intramolecular hydrogen bonding below and above the LCST of 32°C for PNIPAAm. At temperatures above the LCST, the PNIPAAm chains collapse due to increased intramolecular hydrogen bonding between C=O and N–H groups, making it difficult for these hydrophilic C=O and N–H groups to interact with water molecules via intermolecular hydrogen bonding (51).

Surface-Initiated ATRP of PNIPAAm from Silicon Wafers

The ATR-FTIR, AFM, and the water contact angle measurements demonstrate that the surface-initiated ATRP process was successful at modifying the NF 270 membranes with the PNIPAAm and PPEGMA nanolayers. Yet, these characterization tools provide no information about the thicknesses of the polymer nanolayers grafted from the membrane surface. To estimate the layer thickness for a given polymerization time, the nanolayer growth kinetics must be known. In previous work, our group measured the growth kinetics for surface-initiated ATRP of PPEGMA from silicon substrates (9). A flat, reflective substrate allows

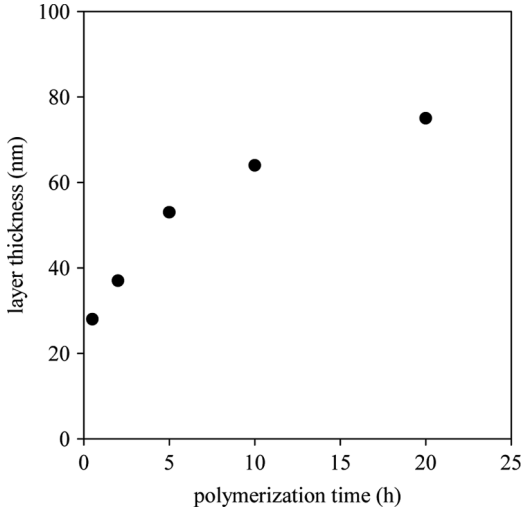

Figure 3. Thickness evolution of surface-initiated PNIPAAm brushes grown from PGMA-modified silicon surfaces having α-bromoester initiator groups.

us to use ellipsometry to measure the nanolayer thickness precisely. In this study, we used ellipsometry to determine the growth kinetics of the surface-initiated ATRP of PNIPAAm.

Silicon substrates were coated with PGMA and then functionalized with an initiator in order to mimic the three-dimensional nature of the initiator incorporation into the membrane surface region. Prior evidence from our group (9,10) suggests that PGMA on silicon serves as a more appropriate model than an initiator monolayer for characterizing the polymer growth kinetics.

PGMA dry layer thicknesses were 9 ± 0.5 nm. The uncertainty represents the standard deviation in thickness among multiple locations on the substrate surfaces. The dry layer thicknesses increased to 11 ± 0.5 nm after the initiator attachment, which was anticipated since mass was added to the layer. Figure 3 shows the thickness evolution for the PNIPAAm nanolayers prepared by the surface-initiated ATRP under the conditions used in this study. The data in Fig. 3 represent the dry layer thicknesses of PNIPAAm only; the thickness of the PGMA + initiator layer was subtracted from the overall thicknesses measured by ellipsometry. Thus, we make the assumption that the layer thicknesses are additive, consistent with the multilayer model used to fit the ellipsometric data.

One characteristic of controlled, surface-initiated ATRP is a linear relationship between the layer thickness and time (22). From Fig. 3, we

see that the conditions used in this study do not yield controlled growth. This result supports the evidence for improper control taken from the AFM roughness measurements on the modified versus the unmodified membranes. A control study was conducted in which a fresh catalyst was added to the system once the layer thickness reached a plateau value. No additional growth occurred; thus, we attribute the nonlinear growth to chain termination (lack of control) and not catalyst deactivation. An additional observation from Fig. 3 is that there is a rapid increase in polymer layer thickness at early polymerization times. This rapid polymer growth is characteristic of water-accelerated ATRP (52). While the controlled growth of substituted acrylamides from surfaces in aqueous media has been reported (20,26–28), the same conditions did not yield control in this work. Controlled polymerization of PNIPAAm by ATRP has been reported in a 50:50 (v/v) dimethylformamide:water mixed solvent system at 20°C (53). Matyjaszewski and co-workers obtained well controlled ATRP of several acrylamides in toluene at room temperature (54,55). However, these latter two solvent systems are not compatible with our polyamide membranes. While controlled growth would improve the reinitiation efficiency for PPEGMA in block copolymer nanolayers, Fig. 3 clearly shows us that chains remain active for relatively long polymerization times. Thus, it is possible to use polymerization time to adjust the nanolayer thickness and still preserve some fraction of chain ends for subsequent reinitiation. On the membrane samples, this result was verified by the ATR-FTIR data in Fig. 1, which show larger peak areas for the membrane that had been modified for longer polymerization times.

Water Flux Measurements to Study Membrane Fouling

Figures 4–7 show water flux through various membranes versus applied pressure. The results are given for the base membrane, as well as NF 270-M2 and NF 270-M4. These membranes are of most relevance in this study as they indicate the effect of grafting PNIPAAm-*block*-PPEGMA to base NF membranes for the shortest and longest modification times that were used. The ATR-FTIR spectrum for NF 270-M3 represents a control that confirms that ATRP successfully grafts diblock copolymer nanolayers from the membrane surface and that increasing grafting time increases the nanolayer thickness. In all cases, water flux increased linearly with increasing pressure. Thus, there appears to be no layer compression under the conditions used for filtration.

Figure 7 compares produced water flux through two modified membranes. Polymer grafting to the membranes led to significant decreases in

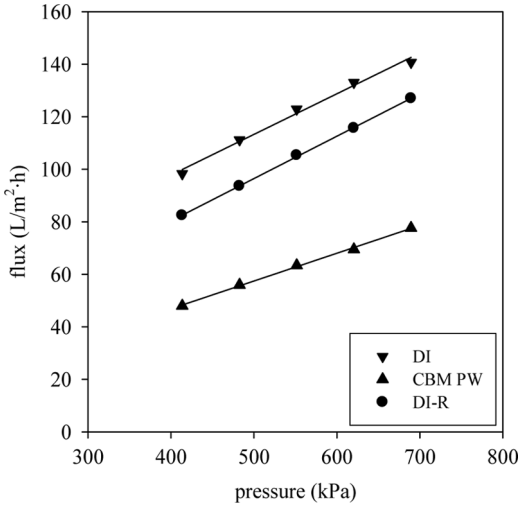

Figure 4. DI and produced water flux through unmodified NF 270 membranes.

flux, but it should be noted that no optimization of polymerization time was done. Long-time polymerizations (2–10 hours for each block) were done to ensure that modification occurred to a significant degree. The estimated thicknesses of the polymer modifying layer are thus

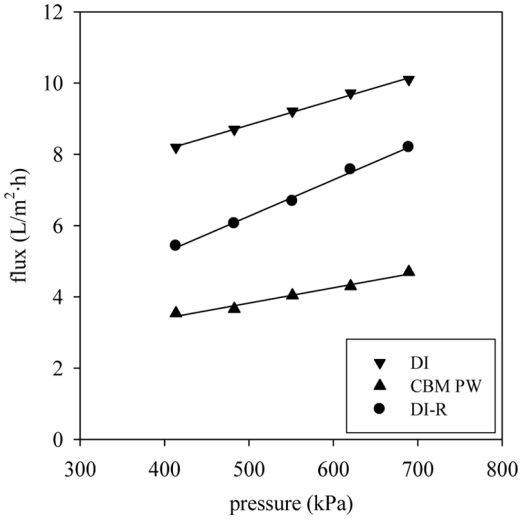

Figure 5. DI and produced water flux through NF 270-M2.

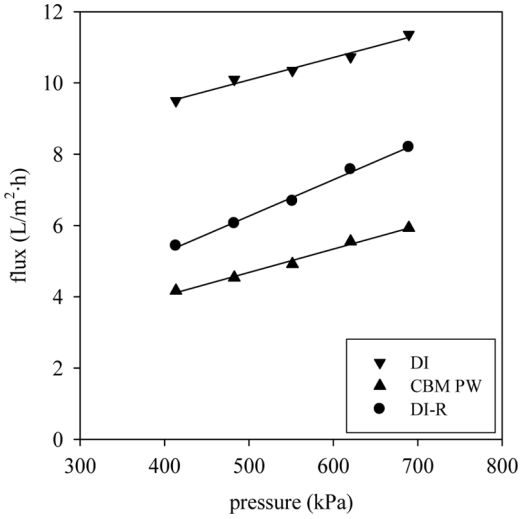

Figure 6. DI and produced water flux through NF 270-M4.

40–90 nm using data from Fig. 3 and a prior publication (9). If polymerization is occurring within the interior pores of the membrane, then these layer thicknesses would lead to pore blocking. A similar conclusion was

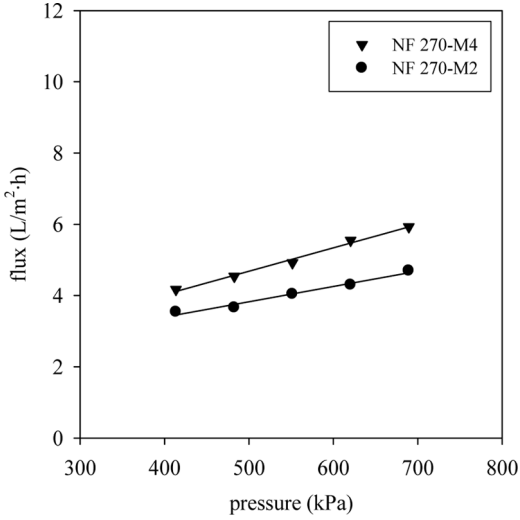

Figure 7. Influence of polymer modifier and graft polymerization times on produced water flux through modified membranes.

drawn by Louie et al. (34) in their work on the physical coating of RO membranes with polyether-*block*-polyamide copolymers. Despite the significant flux loss seen by that group, they found that the slower rate of flux decline for coated membranes compensated for the initial loss in flux, allowing higher volumes of water to be processed over time. We note that our pressure-normalized pure water flux values of $>2\,L \cdot m^{-2} \cdot h^{-1} \cdot bar^{-1}$ compare well with the value of $1.8\,L \cdot m^{-2} \cdot h^{-1} \cdot bar^{-1}$ reported in that work (34).

Comparing PW flux for NF 270-M2 with that for NF 270-M4 in Fig. 7, one can see that longer polymerization times led to lower flux values. Thus, there is an opportunity to use shorter polymerization times (or more open base membranes) to prepare modified membranes with higher flux. Alternatively, one might use a strategy to isolate the surface-initiated polymerization reaction to occur at the membrane surface and prevent it from occurring within the interior pores of the membrane. One such strategy was given by Bruening and coworkers, who physisorbed a polyelectrolyte layer onto alumina membranes having average pore diameters of 20 nm prior to surface-initiated ATRP (12).

Figures 4–6 demonstrate that the flux values of coal bed methane PW (CBM PW) through the membranes are lower than DI water flux for modified and unmodified membranes. After rinsing the membranes with water at 40°C, the recovered DI water flux (labeled as DI-R) is $65 \pm 6\%$ of the original DI water flux for NF 270-M4 and $74 \pm 6\%$ for NF 270-M2. A control test with NF 270-M4 showed that flux recovery was $66 \pm 25\%$ when the water rinse was done at $T < T_{LCST}$ of PNIPAAm. Unmodified NF 270 showed $86 \pm 3\%$ flux recovery. These values compare well with the 85% recovery reported by Kang et al. (35), who challenged the PEG-modified RO membranes with water containing tannic acid/dodecyltrimethylammonium bromide as model contaminants. Louie et al. (34) saw no flux recovery in their long-term study of polyether-*block*-polyamide coated RO membranes challenged with oil/surfactant/water emulsions.

The lower than original DI water flux values result from contaminants that foul the membranes irreversibly. One possible cause for the reduction in flux recovery for modified membranes is that they became more hydrophobic after modification (water contact angle of $49 \pm 2°$ after modification compared to $35 \pm 4°$ for unmodified membranes) (7). The increase in water contact angle stems largely from the PNIPAAm block (contact angle of $61 \pm 2°$). Based on the kinetic data in Fig. 3 and from Singh et al. (9), PNIPAAm has a 7-fold higher growth rate than PPEGMA. Thus, for NF 270-M4, the 2 h polymerization times yield estimated layer thicknesses of 37 nm for PNIPAAm and only 5 nm for PPEGMA. The purpose for attaching the PPEGMA block to the

Table 3. Permeate specifications from filtration of coal bed methane produced water

Membrane	pH	Conductivity (μs)	TDS (ppm)
NF 270	8.54	1297	648
NF 270-M1	8.52	694	342

membrane was to reduce its fouling tendency. In this case, the PPEGMA block may not have been sufficiently thick to prevent access of foulants to the more hydrophobic PNIPAAm layer. Furthermore, the lack of controlled growth for PNIPAAm (Fig. 3) lowers the chain reinitiation efficiency. Therefore, the density of PPEGMA chains in the outer block layer is lower than if polymerization of NIPAAM had been controlled. In prior work (38), we illustrated that higher PPEGMA chain densities improve the resistance of surfaces to biofouling. Thus, improving chain reinitiation efficiency by controlling PNIPAAm growth is an initiative under way in our laboratory. Flux recovery improved for NF 270-M2, which had longer polymerization times, and, therefore, a thicker foul-resistant PPEGMA layer.

Modified membranes did yield better permeate quality compared to unmodified membranes. Table 3 compares quality indicators for permeate collected through unmodified and NF 270-M1 membranes. We have

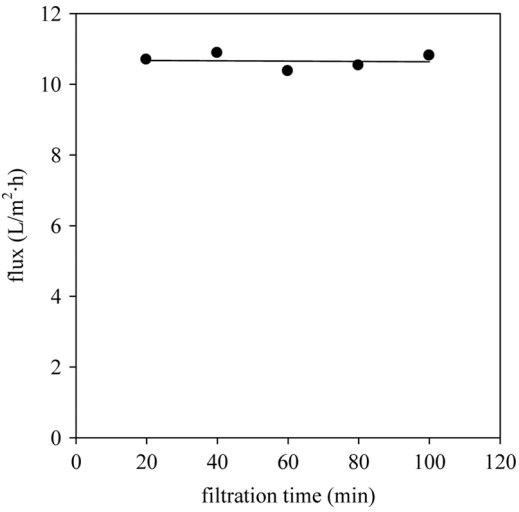

Figure 8. Produced water flux through NF 270-M1 at 550 kPa after rinsing with DI water.

further tested the produced water flux of NF 270-M1 after a second round of DI water filtration. Figure 8 shows the PW flux at constant pressure (550 kPa) as a function of processing time. From Fig. 8, the PW flux remains constant over the 2 h filtration test period. The base NF 270 membrane has the lowest hydrophobicity, while the PNIPAAm modified membrane has the highest hydrophobicity. Based on earlier studies (49) using commercially available NF 270, NF 90, and BW 30 membranes (Dow-FilmTec, Edina, MN), we expect that the small increase in surface roughness after ATRP modification will have a relatively minor effect on fouling compared to the change in hydrophobicity. Since the membrane grafted with only PNIPAAm, M1, shows the greatest increase in hydrophobicity and, hence, the greatest potential for fouling, we compare permeate quality for the base membrane and M1 only. Our results indicate that even for M1, under the experimental conditions investigated, we do observe flux recovery.

CONCLUSIONS

We have demonstrated that room temperature, surface-initiated ATRP can be used to graft PNIPAAm and PNIPAAm-*block*-PPEGMA nanolayers from the surface of polyamide thin-film composite nanofiltration membranes. Modified membranes showed improved permeate water quality relative to unmodified membranes. These membranes maintained constant flux during filtration of coal bed methane produced water.

Contact angle measurements demonstrated the temperature-responsiveness of the modified membranes; however, there was no statistical difference in flux recovery after the produced water filtration and a water rinse step at temperatures above and below the LCST of PNIPAAm. In addition, flux recovery was lower for modified membranes compared to the base membrane, likely attributed to the increase in hydrophobicity after modification. Longer modification time improved flux recovery, as a result of increased PPEGMA layer thickness. Optimization of PPEGMA modification time, combined with controlled growth of PNIPAAm leading to higher chain reinitiation efficiencies, may further improve flux recovery.

The development of low fouling, temperature-responsive NF membranes depends on the ability to reversibly switch membrane hydrophilicity/hydrophobicity with temperature and also the ability to produce membranes with low surface roughness. Our results indicate that surface-initiated ATRP yields lower surface roughness values than other modification methods that graft or physisorb pre-formed polymer chains to the membrane surface.

One hurdle that must be overcome is the significant loss of flux following modification. Along these lines, we show that polymerization time can be varied to adjust the membrane flux. One might also envision using a more open ultrafiltration base membrane for this application. In this way, the polymerization could be used to impart responsive chemistry to the surface and also to "densify" the base membrane. Starting with a more open membrane would allow the optimization of water quality versus flux. Further, while grafting polymer nanolayers from the membrane surface leads to decreases in permeate flux compared to the base membrane, the capacity of the membrane (i.e., the volume of water that can be treated prior to membrane regeneration) is an important consideration for future studies.

ACKNOWLEDGMENTS

We thank the National Science Foundation for financial support under NSF award number CBET 0651646. The authors thank Dr. William Mickols, Dow-FilmTec, Edina, MN for providing the membranes.

REFERENCES

1. Cakmakci, M.; Kayaalp, N.; Koyuncu, I. (2008) Desalination of produced water from oil production fields by membrane processes. *Desalination*, *222* (1–3): 176.
2. Benko, K.L.; Drewes, J.E. (2008) Produced water in the western United States: Geographical distribution, occurrence, and composition. *Environ. Eng. Sci.*, *25* (2): 239.
3. Pimentel, P.M.; Anjos, M.J.; Melo, D.M.A.; Melo, M.A.E.; Goncalves, L.M.; Silva, C.N.; Lopes, R.T. (2008) Multi-elemental analysis of produced water by synchrotron radiation total reflection X-ray fluorescence. *Talanta*, *74* (5): 1231.
4. Mondal, S.; Wickramasinghe, S.R. (2008) Produced water treatment by nanofiltration and reverse osmosis membranes. *J. Membr. Sci.*, *332* (1): 162.
5. Bacchin, P.; Aimar, P.; Field, R.W. (2006) Critical and sustainable fluxes: Theory, experiments and applications. *J. Membr. Sci.*, *281*: 42.
6. Espinasse, B.; Bacchin, P.; Aimar, P. (2008) Filtration method characterizing the reversibility of colloidal fouling layers at a membrane surface: Analysis through critical flux and osmotic pressure. *J. Colloid Interf. Sci.*, *320* (2): 483.
7. Hua, H.L.; Li, N.; Wu, L.L.; Zhong, H.; Wu, G.X.; Yuan, Z.H.; Lin, X.W.; Tang, L.Y. (2008) Anti-fouling ultrafiltration membrane prepared from polysulfone-*graft*-methyl acrylate copolymers by UV-induced grafting method. *J. Environ. Sci-China*, *20* (5): 565.

8. Singh, N.; Wang, J.; Ulbricht, M.; Wickramasinghe, S.R.; Husson, S.M. (2008) Surface-initiated atom transfer radical polymerization: a new method for preparation of polymeric membrane adsorbers. *J. Membr. Sci.*, *309*: 64.
9. Singh, N.; Chen, Z.; Tomer, N.; Wickramasinghe, S.R.; Soice, N.; Husson, S.M. (2008) Modification of regenerated cellulose ultrafiltration membranes by surface-initiated atom transfer radical polymerization. *J. Membr. Sci.*, *311*: 225.
10. Bhut, B.V.; Wickramasinghe, S.R.; Husson, S.M. (2008) Preparation of high-capacity, weak anion-exchange membranes for protein separations using surface-initiated atom transfer radical polymerization. *J. Membr. Sci.*, *325*: 176.
11. Singh, N.; Husson, S.M.; Zdyrko, B.; Luzinov, I. (2005) Surface modification of microporous PVDF membranes by ATRP. *J. Membr. Sci.*, *262*: 81.
12. Balachandra, A.M.; Baker, G.L.; Bruening, M.L. (2003) Preparation of composite membranes by atom transfer radical polymerization initiated from a porous support. *J. Membr. Sci.*, *227*: 1.
13. Friebe, A.; Ulbricht, M. (2007) Controlled pore functionalization of poly(ethylene terephthalate) track-etched membranes via surface-initiated atom transfer radical polymerization. *Langmuir*, *23* (20): 10316.
14. Zhu, L.P.; Dong, H.B.X.; Wei, Z.; Yi, Z.; Zhu, B.K.; Xu, Y.Y. (2008) Tethering hydrophilic polymer brushes onto PPESK membranes via surface-initiated atom transfer radical polymerization. *J. Membr. Sci.*, *320*: 407.
15. Matyjaszewski, K., Xia, J. (2001) Atom transfer radical polymerization. *Chem. Rev.*, *101*: 2921.
16. Edmondson, S.; Osborne, V.L.; Huck, W.T.S. (2004) Polymer brushes via surface-initiated polymerizations. *Chem. Soc. Rev.*, *33*: 14.
17. Werne, T.V.; Patten, T.E. (2001) Atom transfer radical polymerization from nanoparticles: A tool for the preparation of well-defined hybrid nanostructures and for understanding the chemistry of controlled/"living" radical polymerizations from surfaces. *J. Am. Chem. Soc.*, *123*: 7497.
18. Kim, J.B.; Bruening, M.L.; Baker, G.L. (2000) Surface-initiated atom transfer radical polymerization on gold at ambient temperature. *J. Am. Chem. Soc.*, *122*: 7616.
19. Matyjaszewski, K.; Miller, P.J.; Shukla, N.; Immaraporn, B.; Gelman, A.; Luokala, B.B.; Siclovan, T.M.; Kickelbick, G.; Vallant, T.; Hoffmann, H.; Pakula, T. (1999) Radical polymerization in the controlled growth of homopolymers and block copolymers from silicon surfaces in the absence of untethered sacrificial initiator. *Macromolecules*, *32*: 8716.
20. Jayachandran, K.N.; Takacs-Cox, A.; Brooks, D.E. (2002) Synthesis and characterization of polymer brushes of poly(N,N-dimethylacrylamide) from polystyrene latex by aqueous atom transfer radical polymerization. *Macromolecules*, *35*: 4247.
21. Wang, X.S.; Armes, S.P. (2000) Facile atom transfer radical polymerization of methoxy-capped oligo(ethylene glycol) methacrylate in aqueous media at ambient temperature. *Macromolecules*, *33*: 6640.

22. Gopireddy, D.; Husson, S.M. (2002) Room temperature growth of surface-confined poly(acrylamide) from self-assembled monolayers using atom transfer radical polymerization. *Macromolecules*, *35*: 4218.
23. Xiao, D.Q.; Wirth, M.J. (2002) Kinetics of surface-initiated atom transfer radical polymerization of acrylamide on silica. *Macromolecules*, *35*: 2919.
24. Teodorescu, M.; Matyjaszewski, K. (1999) Atom transfer radical polymerization of (meth)acrylamides. *Macromolecules*, *32*: 4826.
25. Rademacher, J.T.; Baum, R.; Pallack, M.E.; Brittain, W.J.; Simonsick, W.J. (2000) Atom transfer radical polymerization of *N,N*-dimethylacrylamide. *Macromolecules*, *33*: 284.
26. Kizhakkedathu, J.N.; Brooks, D.E. (2003) Synthesis of poly(*N*,*N*-dimethylacrylamide) brushes from charged polymeric surfaces by aqueous ATRP: Effect of surface initiator concentration. *Macromolecules*, *36*: 591.
27. Kizhakkedathu, J.N.; Goodman, D.; Brooks, D.E. (2003) Synthesis of poly(*N*,*N*-dimethylacrylamide) brushes from functionalized latex surfaces by aqueous atom transfer radical polymerization. In: *Advances in Controlled/Living Polymerization*; Matyjaszewski, K., ed.; ACS Books: Washington, D.C. Vol. 854; 316.
28. Kizhakkedathu, J.N.; Norris-Jones, R.; Brooks, D.E. (2004) Synthesis of well-defined environmentally responsive polymer brushes by aqueous ATRP. *Macromolecules*, *37*: 734.
29. Heskins, M.; Guillet, J.E. (1968) Solution properties of poly(N-isopropylacrylamide). *J. Macromol. Sci. Chem.*, *A2*: 1441.
30. Schild, H.G. (1992) Poly(N-isopropylacrylamide): experiment, theory and application. *Prog. Polym. Sci.*, *17*: 163.
31. Fujishige, S.; Kubota, K.; Ando, I. (1989) Phase transition of aqueous solutions of poly(N-isopropylacrylamide) and poly(N-isopropylmethacrylamide). *J. Phys. Chem*, *93*: 3311.
32. Schild, H.G.; Tirrell, D.A. (1990) Microcalorimetric detection of lower critical solution temperatures in aqueous polymer solutions. *J. Phys. Chem.*, *94*: 4352.
33. Cho, E.C.; Lee, J.; Cho, K. (2003) Role of bound water and hydrophobic interaction in phase transition of poly(*n*-isopropylacrylamide) aqueous solution. *Macromolecules*, *36*: 9929.
34. Louie, J.S.; Pinnau, I.; Ciobanu, I.; Ishida, K.P.; Ng, A.; Reinhard, M. (2006) Effects of polyether-polyamide block copolymer coating on performance and fouling of reverse osmosis membranes. *J. Membr. Sci.*, *280*: 762.
35. Kang, G.; Liu, M.; Lin, B.; Cao, Y.; Yuan, Q. (2007) A novel method of surface modification on thin-film composite reverse osmosis membrane by grafting poly(ethylene glycol). *Polymer*, *48*: 1165.
36. Kaeselev, B.; Pieracci, J.; Belfort, G. (2001) Photoinduced grafting of ultrafiltration membranes: comparison of poly(ether sulfone) and poly(sulfone). *J. Membr. Sci.*, *194*: 245.
37. Kilduff, J.E.; Mattaraj, S.; Sensibaugh, J.; Pieracci, J.P.; Yuan, Y.X.; Belfort, G. (2002) Modeling flux decline during nanofiltration of NOM with

poly(arylsulfone) membranes modified using UV-assisted graft polymerization. *Environ. Eng. Sci.*, *19*: 477.
38. Singh, N.; Cui, X.; Boland, T.; Husson, S.M. (2007) The role of independently variable grafting densities and layer thicknesses of polymer nanolayers on peptide adsorption and cell adhesion. *Biomaterials*, *28*: 763.
39. Boussu, K.; Zhang, Y.; Cocquyt, J.; Van der Meeren, P.; Volodin, A.; Van Haesendonck, C.; Martens, J.A.; Van der Bruggen, B. (2006) Characterization of polymeric nanofiltration membranes for systematic analysis of membrane performance. *J. Membr. Sci.*, *278*: 418.
40. Kulkarni, A.; Mukherjee, D.; Gill, W.N. (1996) Flux enhancement by hydrophilization of thin film composite reverse osmosis membranes. *J. Membr. Sci.*, *114*: 39.
41. Lui, Y.; Klep, V.; Zdyrko, B.; Luzinov, I. (2004) Polymer grafting via ATRP initiated from macroinitiator synthesized on surface. *Langmuir*, *20*: 6710.
42. Tu, H.; Heitzman, C.E.; Braun, P.V. (2004) Patterned poly(N-isopropylacrylamide) brushes on silica surfaces by microcontact printing followed by surface-initiated polymerization. *Langmuir*, *20*: 8313.
43. Gordon, A.J.; Ford, R.A. (1972) *The Chemists Companion: A Handbook of Practical Data, Techniques and References*; Wiley: New York.
44. Younes, H.; Cohn, D. (1988) Phase separation in poly(ethylene glycol)/poly(lactic acid) blends. *Eur. Polym. J.*, *24*: 765.
45. Yoshida, W.; Cohen, Y. (2003) Topological AFM characterization of graft polymerized silica membranes. *J. Membr. Sci.*, *215*: 249.
46. Freger, V.; Gilron, J.; Belfer, S. (2002) TFC polyamide membranes modified by grafting of hydrophilic polymers: an FT-IR/AFM/TEM study. *J. Membr. Sci.*, *209*: 283.
47. Tanaguchi, M.; Pieracci, J.P.; Belfort, G. (2001) Effect of undulations on surface energy: A quantitative assessment. *Langmuir*, *17*: 4312.
48. Li, X.; Wei, X.; Husson, S.M. (2004) Thermodynamic studies on the adsorption of fibronectin adhesion-promoting peptide on nanothin films of poly(2-vinylpyridine) by SPR. *Biomacromolecules*, *5*: 869.
49. Mondal, S.; Wickramasinghe, S.R. (2008) Produced water treatment by nanofiltration and reverse osmosis membranes. *J. Membr. Sci.*, *322*: 162.
50. Yu, W.H.; Kang, E.T.; Neoh, K.G.; Zhu, S. (2003) Controlled grafting of well-defined polymers on hydrogen-terminated silicon substrates by surface-initiated atom transfer radical polymerization. *J. Phys. Chem. B.*, *107*: 10198.
51. Xie, R.; Chu, L.Y.; Chen, W.M.; Xiao, W.; Wang, H.D.; Qu, J.B. (2005) Characterization of microstructure of poly(N-isopropylacrylamide)-grafted polycarbonate track-etched membranes prepared by plasma-graft pore-filling polymerization. *J. Membr. Sci.*, *258*: 157.
52. Huang, W.X.; Kim, J.B.; Bruening, M.L.; Baker, G.L. (2002) Functionalization of surfaces by water-accelerated atom-transfer radical polymerization of hydroxyethyl methacrylate and subsequent derivatization. *Macromolecules*, *35* (4): 1175.

53. Masci, G.; Giacomelli, L.; Crescenzi, V. (2004) Atom transfer radical polymerization of N-isopropylacrylamide. *Macromol. Rapid Commun.*, *25*: 559.
54. Teodorescu, M.; Matyjaszewski, K. (2000) Controlled polymerization of (meth)acrylamides by atom transfer radical polymerization. *Macromol. Rapid Commun.*, *21*: 190.
55. Neugebauer, D.; Matyjaszewski, K. (2003) Copolymerization of *N*,*N*-dimethylacrylamide with n-butyl acrylate via atom transfer radical polymerization. *Macromolecules*, *36*: 2598.